Electron bubbles in helium clusters. II. Probing superfluidity

Michael Rosenblit[a] and Joshua Jortner[b]
School of Chemistry, Tel Aviv University, Ramat Aviv, 69978 Tel Aviv, Israel

(Received 11 January 2006; accepted 13 March 2006; published online 17 May 2006)

In this paper we present calculations of electron tunneling times from the ground electronic state of excess electron bubbles in $(^4He)_N$ clusters ($N=6500-10^7$, cluster radius $R=41.5-478$ Å), where the equilibrium bubble radius varies in the range $R_b=13.5-17.0$ Å. For the bubble center located at a radial distance d from the cluster surface, the tunneling transition probability was expressed as $A_0\varphi(d,R)\exp(-\beta d)$, where $\beta\simeq 1$ Å^{-1} is the exponential parameter, A_0 is the preexponential factor for the bubble located at the cluster center, and $\varphi(d,R)$ is a correction factor which accounts for cluster curvature effects. Electron tunneling dynamics is grossly affected by the distinct mode of motion of the electron bubble in the image potential within the cluster, which is dissipative (i.e., $\tau_D<\tau_0$) in normal fluid $(^4He)_N$ and $(^3He)_N$ clusters, while it is undamped (i.e., $\tau_D\gg\tau_0$) in superfluid $(^4He)_N$ clusters, where τ_D is the bubble motional damping time ($\tau_D\simeq 4\times10^{-12}$ s for normal fluid clusters and $\tau_D\simeq 10$ s for superfluid clusters), while $\tau_0\simeq 10^{-9}-10^{-10}$ s is the bubble oscillatory time. Exceedingly long tunneling lifetimes, which cannot be experimentally observed, are manifested from bubbles damped to the center of the normal fluid cluster, while for superfluid clusters electron tunneling occurs from bubbles located in the vicinity of the initial distance d near the cluster boundary. Model calculations of the cluster size dependence of the electron tunneling time (for a fixed value of $d=38-39$ Å), with lifetimes increasing in the range of $10^{-3}-0.3$ s for $N=10^4-10^7$, account well for the experimental data [M. Farnik and J. P. Toennies, J. Chem. Phys. **118**, 4176 (2003)], manifesting cluster curvature effects on electron tunneling dynamics. The minimal cluster size for the dynamic stability of the bubble was estimated to be $N=3800$, which represents the threshold cluster size for which the excess electron bubble in $(^4He)_N^-$ clusters is amenable to experimental observation. © *2006 American Institute of Physics*. [DOI: 10.1063/1.2192782]

I. INTRODUCTION

The use of electron bubbles as microscopic probes for superfluidity in bulk liquid ^{4}He dates back to the pioneering 1960 studies of Meyer and Reif.[1] It is of considerable interest to use the electron bubble as a probe for elementary excitations in finite boson quantum systems, i.e., $(^4He)_N$ clusters.[2–8] These clusters are definitely liquid down to 0 K (Refs. 9–11) and, on the basis of quantum path integral simulations,[12,13] were theoretically predicted to undergo a rounded-off superfluid phase transition. A theory of cluster size effects on the λ temperature T_λ in a $(^4He)_N$ cluster[14,15] of radius R resulted in the finite size scaling relation $(T_\lambda^0-T_\lambda)/T_\lambda^0\propto R^{-1/\nu}\propto N^{-1/3\nu}$ for the reduction of T_λ relative to the bulk value $T_\lambda^0=2.17$ K, with $\nu=0.67$ being the critical exponent for the superfluid fraction and for the correlation length in the infinite bulk system.[16] The superfluidity transition and/or Bose-Einstein condensation is exhibited at surprisingly small cluster sizes, i.e., $N_{min}=8-70$,[15] where the threshold cluster size N_{min} is property dependent.[15] The $(^4He)_N$ cluster sizes employed in the experiments of Toennies and co-workers[3,6–8,17,18] and of Northby and co-workers,[4,5] i.e., $N\simeq 10^4-10^7$, are considerably larger than N_{min}. In this large cluster size domain the λ point temperature depression is small,[14,15] i.e., $(T_\lambda-T_\lambda^0)/T_\lambda^0\simeq 2\times10^{-2}-2\times10^{-3}$ for $N=10^4-10^7$. Thus for the current experimentally accessible temperature of 0.4 K, the large $(^4He)_N^-$ clusters ($N=10^4-10^7$) studied by Toennies and co-workers[3,6–8,17,18] are superfluid. On the other hand, $(^3He)_N^-$ clusters studied by Farnik *et al.*[3] correspond to normal fluid clusters. The confrontation between the different features of electron dynamics in superfluid $(^4He)_N^-$ and in normal fluid $(^3He)_N^-$ clusters allowed for the elucidation of the properties of superfluid clusters.[3]

The life story of the excess electron bubble in $(^4He)_N^-$ and $(^3He)_N^-$ clusters is governed by a sequential series of dynamic processes.[15] Following the injection of an excess electron into a helium cluster, the primary dynamic process involves the thermalization of quasi-free electrons.[19] For electrons in the initial kinetic energy range of ~1 keV in macroscopic liquid helium at 1.4 K, the thermalization process occurs on a time scale of 0.3–0.5 ps, with a characteristic stopping distance of $L\sim 50-60$ Å from the surface.[19] The thermalized quasi-free electron undergoes localization via electron bubble formation within the cluster, involving electron localization accompanied by a large configurational dilation, which occurs on the time scale of nuclear motion.[15,20,21] The time τ_b for the electron bubble formation in the center of a helium cluster was estimated[15] by the extension of the theory[20,21] of electron bubble formation in

[a]Present address: Ilse Katz Center for Meso- and Nanoscale Science and Technology, Ben-Gurion University of the Negev, 84105 Beer Sheva, Israel.
[b]Electronic mail: jortner@chemsg1.tau.ac.il

macroscopic liquid helium,[20,21] to include finite cluster size effects and cluster reorganization energy. For superfluid $(^4He)_N$ $(N=1.88\times10^4)$ clusters $\tau_b\simeq4$ ps, while for normal fluid $(^3He)_N$ clusters of the same size $\tau_b\simeq9$ ps, with the relative increase of τ_b in the normal fluid clusters originating from dissipation effects, which are absent in the superfluid clusters.[15,21] Accordingly, on the time scale of $t>\tau_b$ (i.e., $t\gtrsim10$ ps) the equilibrated electron bubble is formed. On this time scale the electron bubble undergoes hydrodynamic motion in parallel with electron tunneling from the bubble.

Electron tunneling dynamics from electron bubbles in helium clusters strongly depends on the nature of the hydrodynamic motion of the electron bubble within the cluster. In normal fluid $(^4He)_N$ and $(^3He)_N$ clusters the electron bubble motion is damped, while in $(^4He)_N$ superfluid clusters this motion is nondissipative.[3] Accordingly, bubble transport dynamics in $(^4He)_N$ clusters dominates the time scale for electron tunneling from the bubble, providing a benchmark for superfluidity in finite boson systems.[8,22] In this paper we address the dynamics of electron tunneling from bubbles in $(^4He)_N$ and $(^3He)_N$ clusters[3,5–8,17,18] and the role of intracluster bubble transport on the lifetime of the bubble states. The problem of electron tunneling dynamics, in conjunction with the bubble motion in the cluster, is of considerable interest, as electron tunneling is expected to be extremely sensitive to the spatial location of the bubble, which is dominated by its hydrodynamic motion. Accordingly, electron tunneling from bubbles will probe superfluidity in ^4He clusters,[8,22] as experimentally demonstrated by Northby and co-workers[4,5] and by Toennies and co-workers.[3,6–8,17] Our work provides semiquantitative information on the dynamics of electron tunneling from bubbles in $(^4He)_N$ clusters, which act as microscopic nanoprobes for superfluidity in finite quantum systems, in accord with the ideas underlying the work of Toennies and co-workers[3,6–8,17] and with the analysis advanced by us,[22] which was referred to by Toennies *et al.* in Ref. 8. A preliminary report of our work was presented.[15] In what follows we provide model calculations of electronic tunneling dynamics coupled to hydrodynamic motion of electron bubbles in $(^4He)_N$ and $(^3He)_N$ clusters.

II. ELECTRON TUNNELING FROM BUBBLES IN $(^4He)_N$ AND $(^3He)_N$ CLUSTERS

Electron emission from bubbles in macroscopic liquid helium was analyzed in terms of electron tunneling through the surface.[23–25] Schoepe and Rayfield[23] advanced a WKB tunneling model through a flat surface, while subsequent studies by Cole and Klein[24] and later by Ancilotto and Toigo[25] calculated the electron escape rates using the Bardeen tunneling Hamiltonian.[26] In order to achieve agreement between theory and experiment, the first calculations[23,24] had to introduce an electron bubble radius of 25 Å which exceeds by about 50% the physical bubble radius of 17–18 Å in the bulk. A more refined analysis by Ancilotto and Toigo[25] attributed this discrepancy to the use of the thermal equilibrium population of electron bubbles, rather than to the stationary concentration, as used by Schoepe and Rayfield[23] and by Cole and Klein.[24] An important conclusion emerging from the analysis of Ancilotto and Toigo[25] is that the electron tunneling probability from the bubble is insensitive to the interface structure of the macroscopic surface and to the structural diffusiveness of the bubble. On the basis of these results[25] we expect that the electron tunneling probability from a bubble in the cluster will be well described in terms of a simplified model, where both the bubble cluster interface and the cluster external interface are sharp.

We present a calculation of the electron tunneling rates from the ground electronic state of electron bubbles of radius R_b in helium clusters of radius R, with the center of the bubble being located at a distance r from the cluster center, with the shortest distance $d=(R-r)$ between the bubble center and the cluster surface. Structural and energetic input information will be based on the results of the accompanying paper[27] (Paper I). The cluster containing the bubble at its equilibrium configuration was represented by a sphere of radius R^e (Paper I), which will be denoted by R in the present paper. The electron bubble was represented by a sphere of the equilibrium radius R_b^e (Paper I), which will be denoted by R_b in the present paper. The interior density profile of the bubble (Paper I) will be approximated by a sharp boundary. We could attempt to replace the bubble radius R_b by an effective radius to account for the effects of the interior density profile. However, in view of incomplete information regarding the initial values of the cluster surface initial distance d (Ref. 19 and Sec. V below), this is not necessary at present. d and the barrier width $d-R_b$ will be taken as parameters of the theory. Calculations for the structure and energetics of the electron bubble in the vicinity of the surface of macroscopic liquid helium[25] reveal that the bubble radius and the electronic energy weakly depend on the bubble-surface distance for $d>23$ Å, being in the range that is of interest to us. In our analysis of electron tunneling lifetimes from bubbles in helium clusters (Secs. III–V below) we shall be interested in the range of $d=30-50$ Å, whereupon the invariance of R_b and the electronic energy with respect to the variation of d will be invoked.

The tunneling process is characterized by a barrier height of V_0-E_e, which is given by the energy gap between the quasi-free electron energy V_0 and the electronic energy E_e of the ground electronic state at the bubble equilibrium configuration (Paper I), and by barrier widths $(X-R_b)$, where the distance X from the center of the bubbles to some point on the cluster surface is $X\geqslant d$. The tunneling probability $F(X)$ is approximated by the WKB expression

$$F(X)=\nu\exp(-2\alpha X), \tag{1}$$

where

$$\alpha=[(2m_e/\hbar^2)(V_0-E_e)]^{1/2} \tag{2}$$

and the tunneling frequency is

$$\nu=(2V_0/m_e)^{1/2}/2R_b. \tag{3}$$

The tunneling transition rate through a solid angle $d\Omega$ is $F(X(\Omega))d\Omega/4\pi$, where $X(\Omega)$ depends on the angular coordinates, while the total tunneling transition rate is

$$\phi(d) = \nu \int_{\Omega} F(X(\Omega))d\Omega/4\pi. \tag{4}$$

The general form of the total transition rate, Eq. (4), is expected to be of the form

$$\phi(d) = A\exp(-\beta d), \tag{5}$$

where A is the preexponential factor and $\beta=2\alpha$ is the exponential parameter. Equation (5) manifests the common exponential distance dependence of electron tunneling processes.

For electron tunneling from a "helium balloon," i.e., from a bubble located at the center of the cluster where $d=R$ and $X(\Omega)=(R-R_b)$ for all values of Ω, Eqs. (2)–(4)result in the simple form of the parameters in Eq. (5), $\beta=2\alpha$, where α is given by Eq. (2), and $A=A_0$, where

$$A_0 = (V_0/2m_eR_b^2)^{1/2}\exp(2\alpha R_b). \tag{6}$$

We compare electron tunneling rates from a bubble located in the center of the cluster, Eqs. (5) and (6), with a bubble whose center is displaced from the cluster center, i.e., $d<R$. The latter case will be characterized by the same exponential parameter $\beta=2\alpha$, while the preexponential factor A will be reduced relative to the value of Eq. (6). Accordingly, for the general case of electron tunneling from a bubble in a cluster we set

$$\beta = 2\alpha \tag{7a}$$

and

$$A = \varphi(d,R)(V_0/2m_eR_b^2)^{1/2}\exp(2\alpha R_b), \tag{7b}$$

where $A=A_0\varphi(d,R)$ and $\varphi(d,R)$ is the correction factor for the displacement of the bubble center from the cluster center.

We now consider electron tunneling rates from a bubble, which is displaced from the center of the cluster. The origin of the coordinate axes will be taken at the cluster center and the center of the bubble is taken at $r=R-d$ on the z axis. The distance $X(\theta)$ from the center of the bubble to a point specified by the polar coordinates (R,θ,ϕ) on the cluster surface (inset to Fig. 1) is given by

$$X(\theta) = [d^2 + 2(R^2 - Rd)(1-\cos\theta)]^{1/2}. \tag{8}$$

The tunneling rate, Eq. (4), is

$$\phi(d,R) = (\nu/2)\int_0^{\pi} d\theta \sin\theta \exp[-\beta(X(\theta) - R_b)]. \tag{9}$$

The integration in Eq. (9) with $X(\theta)$ given by Eq. (8) results in

$$\begin{aligned}\phi(d,R) = {} & \nu\exp(\beta R_b)[1/\beta^2(R^2 - Rd)] \\ & \times\{\exp(-\beta d)(\beta d+1) - \exp[-\beta(d^2 + 4R^2 \\ & - 4Rd)^{1/2}][\beta(d^2 + 4R^2 - 4Rd)^{1/2} + 1]\},\end{aligned} \tag{10a}$$

where $\beta=2\alpha$, [Eq. (7a)]. Equation (10a) can be recast in the form of Eq. (5) with the correction factor in Eq. (7b) being given by

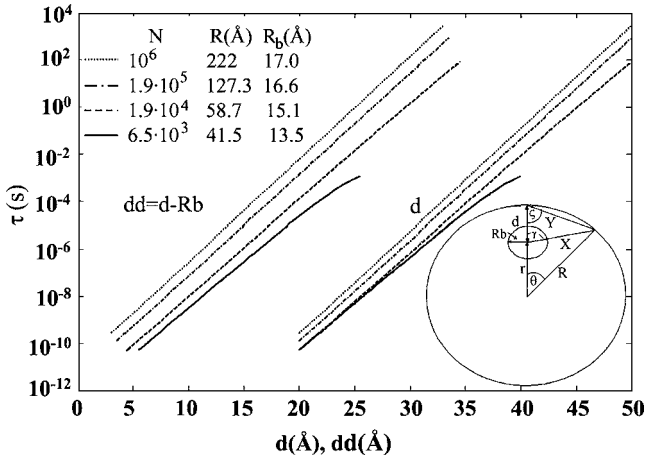

FIG. 1. Electron tunneling lifetimes $\tau=1/\phi(d)$ from electron bubbles whose center is located at the shortest distance $d=R-r$ from the cluster surface and whose shortest tunneling barrier is $dd=d-R_b$. Data are given for cluster sizes $N=6.5\times10^3$, 1.4×10^4, 1.9×10^5, and 10^6, with the corresponding equilibrium bubble radii R_b and the cluster radii R being marked on the panel. The four lines on the RHS of the panel correspond to the τ vs d dependence, while the four lines on the LHS of the panel correspond to the τ vs dd dependence. Note the near-exponential dependence of τ on d and on dd for the fixed value of N (and R). The inset on the lower RHS of the panel presents the geometrical parameters for the model.

$$\begin{aligned}\varphi(d,R) = {} & (\beta d+1)/[\beta^2(R^2 - Rd) - \exp(-2\beta(R-d))] \\ & \times[(\beta(2R-d)+1)/(\beta^2(R^2 - Rd))].\end{aligned} \tag{10b}$$

Equation (10a) is useful for moderately small clusters ($N\leqslant10^4, R\leqslant55$ Å) when the bubble radius approaches the cluster radius. Larger clusters ($N=1.88\times10^5-10^7$ with $R=127-477$ Å) are of interest in the context of electron tunneling from the bubble at $d\leqslant50$ Å,[19] so that the shortest barrier width is $d-R_b\leqslant35$ Å, which is lower than the cluster radius, i.e., $(d-R_b)\ll R$ and $d/R=0.05-0.5$. In this small d/R expansion limit, it will be convenient to express Eqs. (10a) and (10b) in the alternative form

$$\begin{aligned}\phi(d,R) = {} & \nu\exp(\beta R_b)\{\beta^2R^2[1-(d/R)]\}^{-1} \\ & \times\{\exp(-\beta d)(\beta d+1) - \exp[-\beta R[(d^2/R^2)+4 \\ & - 4(d/R)]^{1/2}][\beta R[(d^2/R^2)+4-4(d/R)]^{1/2}+1]\}.\end{aligned} \tag{11}$$

For the range of $d/R\leqslant0.5$ and $\beta d\gg1$, Eq. (11) reduces to

$$\begin{aligned}\phi(d,R) = {} & \exp(-\beta d)\exp(\beta R_b)[1/(\beta d)](d/R)^2/ \\ & [1-(d/R)].\end{aligned} \tag{12a}$$

The correction factor, $\varphi(d,R)$ [Eq. (7b)], for the preexponential factor in the tunneling process accompanying the displacement of the bubble center from the cluster center towards the cluster surface, i.e., $d\sim(0.1-0.5)R$, is

$$\varphi(d,R) = [1/(\beta d)](d/R)^2/[1-(d/R)]. \tag{12b}$$

Two limiting results emerge from the present analysis of electron tunneling from bubbles in clusters.

(1) Electron tunneling from a "helium balloon" with the bubble being located at the center of the cluster ($d=R$). In the limit when the bubble approaches the cluster center, i.e., $\delta=R-d\ll R$, we define a parameter

$$a = 2[(R/d)^2 - (R/d)] \tag{13}$$

for the expansion near $d \sim R$, which in this limit corresponds to $a \simeq 2(\delta/R) \ll 1$. Equation (10a) then assumes the form

$$\phi(d,R) = \nu \exp(\beta R_b)(1/\beta^2 d^2 a)\{[\exp(-\beta d)(\beta d+1)] - \exp[-\beta d(2a+1)^{1/2}][\beta d(2a+1)^{1/2}+1]\}. \tag{14}$$

The expansion of Eq. (14) in powers of a results in

$$\phi(d,R) = \nu \exp(\beta R_b)\exp(-\beta R) + O(a^2), \tag{15}$$

which converges to the expression for electron tunneling from a bubble located at the center of the cluster [Eqs. (5) and (6)].

(2) Electron tunneling from a bubble located near a flat surface. At this stage it will be useful to specify the distance $Y(\theta)$ between the surface points $(R, \theta=0)$ and $R(\theta)$ (inset to Fig. 1),

$$Y(\theta) = R[2(1-\cos\theta)]^{1/2}. \tag{16}$$

The distances $X(\theta)$ and $Y(\theta)$ can alternatively be characterized by the angle γ between **x** and **d** and the angle $\zeta = (\pi - \theta)/2$ (inset to Fig. 1) in the form

$$Y(\gamma) = [d^2 + X^2 - 2dX\cos\gamma]^{1/2} \tag{17}$$

and

$$X(\zeta) = (Y^2 + d^2 - 2dY\cos\zeta)^{1/2}. \tag{18}$$

From Eqs. (8) and (16)–(18) we infer that

$$X = (d - Y\cos\zeta)/\cos\gamma \tag{19a}$$

and

$$\cos\theta = 1 - Y^2/2R^2. \tag{19b}$$

For $R \to \infty$, Eq. (19b) yields $\cos\theta = 1 (\theta = 0)$, so that $\cos\zeta = 0 (\zeta = \pi/2)$. Equation (19a) then results in

$$X = d/\cos\gamma. \tag{20}$$

From Eqs. (1), (4), and (20) one obtains the transition probability through a flat surface,

$$\phi(d, R=\infty, \theta=0, \xi=\pi/2) = (V_0/2m_e R_b^2)^{1/2}\exp(2\alpha R_b)\exp(-2\alpha R) \times \exp(-1/\alpha d)/(4\alpha d). \tag{21}$$

Equation (21) reproduces the Schoepe-Rayfield equation.[23] Equation (21) is again expressed in the form of Eq. (5) with the preexponential factor

$$A = (V_0/2m_e R_b^2)^{1/2}\exp(2\alpha R_b)\exp(-1/\alpha d)/(4\alpha d), \tag{22a}$$

and the correction factor, Eq. (7b), is

$$\varphi(d, R\to\infty, \theta=0, \xi=\pi/2) = \exp(-1/\alpha d)/(4\alpha d). \tag{22b}$$

The flat surface correction factor φ, Eq. (22b), is finite, being independent of R. We note in passing that this flat surface result differs from the spherical cluster result, Eq. (10b), which manifests the effects of surface curvature, i.e., a finite value of θ.

From our results the following conclusions emerge.

(1) The main contribution to the dependence of the tunneling transition probability $\phi(d,R)$ on the bubble center-cluster surface shortest distance d is manifested by the exponential dependence $\exp(-\beta d)$, Eqs. (5) and (7a), with $\beta \simeq 1$ Å^{-1} (Sec. III). The preexponential factor A and the correction factor, Eq. (7b), exhibit an algebraic distance dependence on d and on R.

(2) In general, $\varphi(R,d) \leqslant 1$, with $\varphi(R, d=R) = 1$. The correction factor, Eq. (7b), manifests the reduction of the preexponential factor for moving the bubble away from the cluster center.

(3) The displacement of the bubble center from the cluster center at a fixed value of d (which is accomplished by increasing the cluster radius R) will result in the decrease of the correction factor $\varphi(d,R)$ with increasing R, according to Eqs. (10b) and (12b), e.g., $\varphi(d,R) = (d/R)^2/[1-(d/R)]$ for $d/R = 0.05-0.5$. Consequently, as the exponential contribution to $\phi(R,d)$ is constant (at a fixed value of d), the transition probability for tunneling decreases with increasing R. This reduction manifests cluster surface curvature effects on the tunneling transition probability.

(4) The extreme case of the absence of surface curvature effects is exhibited for tunneling through a flat, macroscopic surface, Eqs. (21), (22a), and (22b). The correction factor, Eq. (22b), for $\alpha d \gg 1$ is $\varphi = [1 - 1/\alpha d]/4\alpha d$. This result manifests the limits $R/Y \to \infty$, $\theta = 0$, and $\zeta = \pi/2$, exhibiting an algebraic reduction factor of $\varphi \propto 1/d$ for the flat surface. On the other hand, for very large spherical clusters $\varphi \propto 1/R^2 \to 0$ when $R \to \infty$, preserving the effects of surface curvature.

(5) The displacement of the bubble center towards the cluster surface at a fixed value of the cluster radius R results in a marked enhancement of the electron tunneling probability. This increase of $\phi(R,d)$ with decreasing d originates from the dominating strong exponential increase of $\phi(R,d)$, which occurs concurrently with the algebraic-type decrease of the correction factor $\varphi(R,d) \propto d$ and of the preexponential factor A with decreasing d.

III. ELECTRON TUNNELING TIMES

The electron tunneling times τ from a bubble whose center is located at a distance d from the cluster surface are given by

$$\tau = 1/\phi(d,R), \tag{23}$$

where from Eqs. (5), (6), (7a), and (7b)

$$\tau = A_0^{-1}\varphi(d,R)^{-1}\exp(\beta d). \tag{24}$$

The tunneling lifetimes were calculated from Eqs. (2), (6), (7a), (7b), (10a), (10b), and (24) in the cluster size domain $N = 6.5\times10^3 - 10^7$. The cluster radii (in the presence of the equilibrium configuration of the electron bubble, which is located at the center of the cluster), vary in the range

TABLE I. Structural, energetic, and dynamic parameters for electron tunneling from $(^4He)_N$ clusters.

N	R[a] (Å)	V_0-E_e[a] (eV)	R_b[a] (Å)	β[b] (Å^{-1})	A[c] (10^{19} s^{-1}) d=38 Å	A[c] (10^{19} s^{-1}) d=39 Å	$\varphi(d,R)$[d] d=38 Å	$\varphi(d,R)$[d] d=39 Å
6.5×10^3	41.5	0.790	13.5	0.998	10.31	14.71	0.27 (0.13)	0.38 (0.19)
1.84×10^4	58.7	0.854	15.1	1.014	3.99	4.30	3.2×10^{-2} (1.9×10^{-2})	3.4×10^{-2} (2.0×10^{-2})
1.88×10^5	127.3	0.908	16.6	1.029	2.10	2.18	3.3×10^{-3} (2.5×10^{-3})	3.5×10^{-3} (2.6×10^{-3})
10^6	222.0	0.930	17.0	1.039	0.76	0.79	9.2×10^{-4} (7.6×10^{-4})	9.5×10^{-4} (7.9×10^{-4})
10^7	478.0	0.934	17.0	1.039	0.15	0.15	1.8×10^{-4} (1.6×10^{-4})	1.8×10^{-4} (1.7×10^{-4})

[a]Data from Paper I (Ref. 27).
[b]$\beta=2\alpha$, Eq. (2).
[c]The preexponential factor A, Eqs. (7b) and (10b). Data for d=38 Å and d=39 Å.
[d]The correction factors $\varphi(d,R)$, Eq. (10b). The approximate correction factors, calculated from Eq. (12b), which are valid for $d/R<0.5$ and $\beta d\gg1$, are presented in parentheses. The correction factors are given for d =38 Å and d=39 Å.

R=41.5 Å for $N=6.5\times10^3$ (R_b=13.5 Å), R=58.7 Å for $N=1.86\times10^4$ (R_b=15.1 Å), and R=127.3 Å for $N=1.88\times10^5$ (R_b=16.6 Å) to R=222 Å for $N=10^6$ (R_b=17.0 Å).[27] The shortest bubble center-cluster surface distance $d=R-r$ (inset to Fig. 1) was varied in the range d=20–38 Å for $N=1.4\times10^4-10^7$ and d=20–50 Å for $N=6.5\times10^3$. These values of d determine the widths of the tunneling barrier $dd=d-R_b$. The cluster radii R and the bubble radii R_b were taken from the structural data presented in Paper I.[27] Furthermore, we assumed that R and R_b, which were calculated for the electron bubble located at the center of the cluster, are invariant with respect to the displacement of the electron bubble within the cluster. At a fixed cluster size τ exhibits a near-exponential dependence on d (Fig. 1). According to Eq. (24), this is dominated by the exponential term $\tau\propto\exp(\beta d)$. The parameter β weakly varies in the range $\beta=0.998-1.039$ Å^{-1}, due to the change of the barrier energy (V_0-E_e) (Table I), which determines $\beta=2\alpha$, according to Eq. (2). An additional contribution to the d dependence of τ (at fixed R and R_b) originates from the correction factor $\varphi(d,R)$, i.e., $\tau\propto[\phi(d,R)]^{-1}$, according to Eqs. (10b) and (12b). $\varphi(d,R)$ increases with increasing d at a fixed value of R, due to cluster curvature effects (Sec. II), with τ being somewhat shortened with increasing d. These cluster curvature effects on τ are most pronounced for the bubble center located near the cluster center in the smallest cluster ($N=6.5\times10^3$, R=41.5 Å) studied herein (Fig. 1), where the tunneling lifetimes exhibit a negative deviation from the exponential d dependence. In the range d=35–40 Å, at a fixed value of d, we found that τ increases by about a numerical factor of ~50 between the cluster sizes $N=6.5\times10^3$ and $N=10^6$ (Fig. 1). The major contribution to this increase of τ with increasing R (at a fixed value of d) originates from the cluster size dependence of the preexponential factor (Table I), with A^{-1} increasing by a numerical factor of ~15–20 with increasing R in the range R=41.5–222 Å. This contribution to the increase of A^{-1} originates from the correction factor $\varphi(d,R)^{-1}$, Eq. (10b), and can be traced to cluster curvature effects on the tunneling lifetime. A second, modest contribution to the increase of τ with increasing R (at a fixed value of d) originates from the increase of the exponential parameter β with increasing R (Table I). The variation of β by $\Delta\beta$=0.04 Å in the size domain $N=6.5\times10^3-10^6$ results in the additional lengthening of τ by a numerical factor of $\exp(\Delta\beta d)\simeq5$ at d=38 Å.

In Table I we summarize the dynamic parameters β, A, and $\varphi(d,R)$, which determine the lifetimes, Eq. (24), of electron tunneling from $(^4He)_N$ clusters. The increase of the exponential parameter $\beta=2\alpha$ with increasing R originates from the change of the energy barrier. The preexponential factor A, Eq. (7b), exhibits a marked cluster size dependence, due to two effects: (i) the increase of A_0, Eq. (6), with increasing R, which can be traced to its dependence on the bubble radius R_b, according to Eq. (7b), and (ii) the decrease of the correction factor $\varphi(d,R)$ at a fixed distance d, Eq. (10b), with increasing R (Table I). With increasing R, the composite contributions of A_0 and $\varphi(d,R)$ to A result in its net decrease for a larger cluster size (Table I). For $N\geqslant1.84\times10^4$ ($R\geqslant59$ Å) the correction factor $\varphi(d,R)$, calculated from Eq. (12b), is in good agreement with the approximate correction factor calculated from Eq. (15), expected to be valid for $d/R<0.5$ and $\beta d\gg1$ (Table I). For the smaller cluster of $N=6.5\times10^3$ a deviation of ~30% between the "exact" and the approximate results is exhibited and the former data should be used. To complete these data, we have performed model calculations for electron tunneling lifetimes from $(^3He)_N$ clusters. For example, for a cluster with $N=10^6$ (R =242 Å), R_b^e=19.0 Å, V_0=0.90 eV, and E_e^e=0.077 eV.

The relevant spatial range of the d values for the initial location of the bubble can be inferred from the characteristic spatial range $L\sim50$ Å for thermalization of electrons in macroscopic liquid helium,[19] which constitutes an upper limit for d. The lower limit for d is due to the experimental limitations on the time scale for electron detection of the

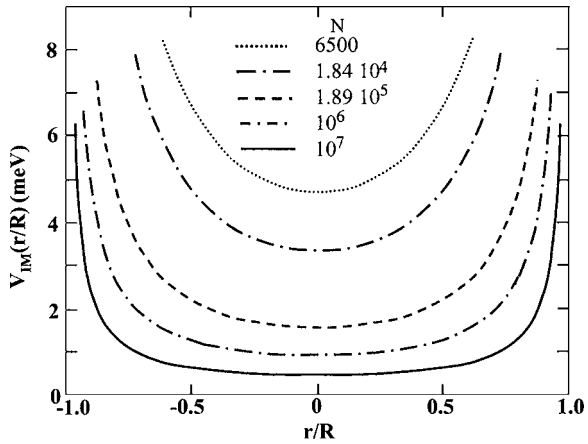

FIG. 2. The image potential $V_{\rm im}(r;R)$, Eq. (25), for the motion of an electron bubble in $(^4{\rm He})_N$ for several cluster sizes presented on the curves. The image potentials are presented in the reduced coordinates r/R.

$(\mathrm{He})_N^-$ ions, which fall in the range of $t>10^{-6}$ s. The corresponding distance for electron tunneling of $\tau=10^{-6}$ s inferred from Fig. 1 is $d_{\rm min}=30-32$ Å. We thus expect the d values for the interrogation of tunneling from electron bubbles to fall in the physically acceptable region $d_{\rm min}=30$ Å $\leqslant d \leqslant L \simeq 50$ Å.

IV. ELECTRON BUBBLE MOTION IN THE IMAGE POTENTIAL WITHIN $(\mathrm{He})_N$ CLUSTERS

The electron bubble motion within the cluster is described to occur in the image potential well $V_{\rm im}(r)$, which is given by[27]

$$V_{\rm im}(r;R)=(2\Sigma/R)\{(1-(r/R)^2)^{-1}+(R/2r) \times \ln[(R+r)/(R-r)]\}, \tag{25}$$

where $r=(R-d)$ and $\Sigma=e^2(\varepsilon-1)/4\varepsilon(\varepsilon+1)$. $V_{\rm im}(r;R)$ is the cluster polarization potential outside the bubble in the limit $R_b=0$. Equation (25) is obtained from Eq. (22) of Paper I, setting $\beta=0$. For the electron bubble located in the center of the cluster, i.e., $d=R$, $V_{\rm im}(r=0;R)$ is of the form $V_{\rm im}(r=0;R)\propto 1/R$. It will be useful to recast the image potential, Eq. (25), in the form

$$V_{\rm im}(r;R)=V_{\rm im}(r=0;R)+\bar{V}_{\rm im}(r,R). \tag{26}$$

In Fig. 2 we portray the dependence of the image potentials on the initial distance r from the cluster center for $(^4{\rm He})_N$ clusters in the size domain $N=6.5\times10^3-10^6$. In our treatment it will be implicitly assumed that the ground state electronic energy, the cluster deformation energy accompanying bubble formation, and the equilibrium bubble radius exhibit a weak dependence on d. Then the energetic changes accompanying the displacement of the bubble center within the cluster solely result from the contribution of the image potential. Following the localization of the quasi-free electron at the distance $d=R-r$ from the cluster surface, where the bubble is initially formed, the electron bubble will move in the image potential well. Two limiting cases involving distinct modes of the electron bubble motion within the image potential, which is dissipative in normal $(^4{\rm He})_N$ $(T>T_\lambda)$ clusters and in $(^3{\rm He})_N$ clusters and is nearly undamped in superfluid $(^4{\rm He})_N$ clusters $(T\ll T_\lambda)$, will now be considered.

The bubble translational dynamics at distance r from the cluster center will be described by an approximate, one-dimensional, Langevin equation of motion,

$$M_b\ddot{r}+\partial V_{\rm im}(r)/\partial r+4\pi\eta R_b\dot{r}=0, \tag{27}$$

where M_b is the effective mass of the electron bubble of radius R_b, which involves the near external layers of the He atoms (of mass in $m_{\rm He}$), taken from the experimental data[28] as $M_b\simeq 240 m_{\rm He}$. η is the viscosity of the fluid, which varies dramatically between the normal fluid [$\eta=200$ μP (Ref. 29)] and the superfluid.[25] A rough estimate of η for the macroscopic superfluid can be inferred[25] from the Einstein-Stokes relation, which yields $\eta=e/6\pi R_b\mu$, where $\mu=8.62\times10^{-4}\exp(8.45/T)$ cm^2 V^{-1} s^{-1} is the bubble mobility[25] at $T=0.4$ K.[30–35] This estimate results in $\eta\approx10^{-10}$ μP for the superfluid. $V_{\rm im}(r)$ is the image potential, Eq. (26), with the second term on the left-hand side (LHS) of Eq. (27), $\partial V_{\rm im}(r)/\partial r$, being the restoring force. An approximate representation of the image potential as a harmonic potential with force constant k and restoring force $-kr$, i.e., $V_{\rm im}(r)\simeq V_{\rm im}(0)+kr^2/2$, results in the crude values of $k=0.15$ erg cm^{-2} for $N=6.5\times10^3$ and $k=1.3\times10^{-3}$ erg cm^{-2} for $N=10^6$. The third term on the LHS of Eq. (27) represents the drag force.

The solution of the equation of motion, Eq. (27), is of the form

$$r(t)=A\exp(\alpha_1 t)+B\exp(\alpha_2 t), \tag{28a}$$

with

$$\alpha_{1,2}=-(1/2\tau_D)\pm[(1/2\tau_D)^2-(1/\tau_0)^2]^{1/2}, \tag{28b}$$

where the damping time inferred from Stokes law is

$$\tau_D=M_b/4\pi\eta R_b, \tag{29a}$$

while the oscillation time in the image potential is

$$\tau_0=(M_b/k)^{1/2}, \tag{29b}$$

with the oscillation period of $2\pi\tau_0$.

The solution of the equation of motion, Eq. (27), can be recast in an alternative form describing a damped oscillatory motion,

$$r(t)=r(0)\exp(-t/2\tau_D)\exp(it/\bar{\tau}_0), \tag{30}$$

where τ_D is given by Eq. (29a) and $\bar{\tau}_0=[(1/\tau_0)^2-(1/2\tau_D)^2]^{-1/2}$. In the overdamped regime, when $\tau_0^2\gg(2\tau_D)^2$, $r(t)\simeq r(0)\exp(-t/\tau_D)$, while in the underdamped region, when $\tau_0^2\ll(2\tau_D)^2$, $r(t)\simeq r(0)\exp(it/\tau_0)$.

Typical values of the oscillation times τ_0, Eq. (29b), obtained from the crude values of k estimated above, are $\tau_0=9.5\times10^{-11}$ s for $N=6500$ $(R=41.5$ Å) and $\tau_0=1.0\times10^{-9}$ s for $N=10^6$ $(R=222$ Å). A rough estimate of the damping lifetime τ_D, Eq. (29a), for the normal fluid is[3] $\tau_D=4\times10^{-12}$ s. The oscillation times, Eq. (30), for $N=6500-10^6$ fall in the range $\tau_0=10^{-10}-10^{-9}$ s. Accordingly, in the normal fluid $\tau_D\ll\tau_0$, and Eqs. (28a) and (28b) result in

$$r(t) = \exp(-t/\tau_D). \tag{31}$$

The bubble motion in the normal fluid, Eq. (31), will be overdamped. The bubble will then relax to the cluster center on the time scale of τ_D, which is short relative to the electron tunneling time from the normal fluid cluster. Accordingly, electron tunneling from bubbles in normal liquid clusters of helium will occur from a thermally equilibrated position of the bubble.

For the bubble motion in the image potential with the superfluid, one infers that for the experimentally relevant temperature of 0.4 K,[3,6–8,17,18,30–35] only the superfluid component is expected to prevail in the cluster size domain ($N > 10^3$) which is of interest to us. The drag force acting on the electron bubble in superfluid $(^4\mathrm{He})_N$ clusters is expected to be vanishingly small due to the negligible viscosity [i.e., $\eta \lesssim 10^{-9}-10^{-11}$ μP (Ref. 25)], whereupon the damping time, Eq. (29a), is $\tau_D \simeq 10$ s. τ_D is larger by about ten orders of magnitude than the bubble oscillation time, Eq. (30), $\tau_0 = 10^{-9}-10^{-10}$ s. As $\tau_0 \ll 2\tau_D$ for the superfluid, Eqs. (28a) and (28b) result in

$$r(t) = \exp(it/\tau_0). \tag{32}$$

The exceedingly long damping time marks the negligible dissipation motion of the bubble, which will undergo oscillatory motion. The separation of time scales between fast oscillation and extremely long damping allows to consider electron tunneling from the bubble, which oscillates within the superfluid cluster.

V. ELECTRON TUNNELING TIMES

A. Slow electron tunneling from normal fluid helium clusters

From the foregoing analysis in Sec. IV we concluded that in normal fluid $(^4\mathrm{He})_N$ or $(^3\mathrm{He})_N$ clusters the electron bubble will relax to the cluster center on the time scale of the damping time $\tau_D \sim 4\times 10^{-12}$ s. Furthermore, for $d > 20$ Å (see Fig. 1), the electron tunneling times, Eq. (23), are longer than the damping times, i.e., $\tau > \tau_D$. Accordingly, the electron tunneling times ($\tau > 10^{-6}$ s) in the physically acceptable region 30 Å $\leqslant d \leqslant$ 50 Å (Sec. IV) are considerably longer than τ_D. For this physically acceptable d domain the electron bubble motion in the normal fluid cluster is overdamped towards the equilibrium configuration in the center of the cluster. The bubble relaxes to the minimum of the image potential, which is located in the vicinity of $r=0$ (Fig. 2), without electron escape during the translational relaxation. Subsequently, electron tunneling from the centrally located electron bubble, i.e., from an electron in the helium balloon, will prevail. The electron bubble configurational distribution $p_s(r)$ in the image potential within the cluster prior to electron tunneling was taken in the form of an equilibrium Boltzmann distribution in the absence of tunneling, which is described by the static approximation[4,5]

$$p_s(r) = (1/2)\exp(-\bar{V}_{\mathrm{im}}(r)/k_B T). \tag{33}$$

The time dependent survival probability $I(t)$ of the electron bubble in the cluster is given by

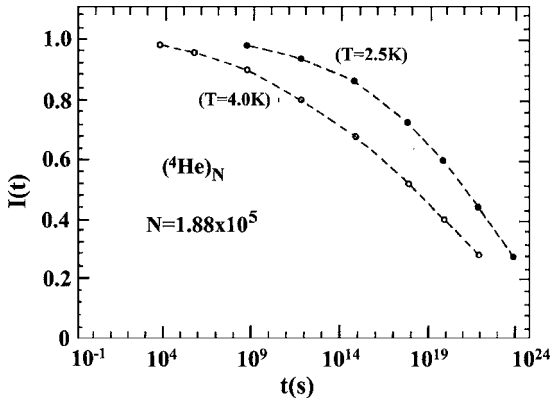

FIG. 3. The electron bubble survival probability $I(t)$, Eqs. (33) and (34), from a bubble located near the center of the normal fluid $(^4\mathrm{He})_N$ clusters ($N = 1.88\times 10^5$, $R = 127$ Å), at different temperatures ($T > T_\lambda$) marked on the curves.

$$I(t) = \int_0^R p_s(r)\exp(-\phi(r)t)dr \Big/ \int_0^R p_s(r)dr, \tag{34}$$

where $\bar{V}_{\mathrm{im}}(r)$ is given by Eq. (26) and $\phi(r)$ is given by Eqs. (10a) and (11). In Figs. 3 and 4 we portray typical $I(t)$ versus t curves calculated from Eqs. (33) and (34) for normal fluid $(^4\mathrm{He})_N$ clusters at $T=2.5$ and 4.0 K (Fig. 3) and for normal fluid $(^3\mathrm{He})_N$ clusters at $T=0.4$, 1.25, and 4.0 K (Fig. 4). The $I(t)$ versus t curves are exponential for $(^3\mathrm{He})_N$ clusters at $T=0.4$ K, while for higher temperatures of $T=3-4$ K the $I(t)$ versus t curves are nonexponential, being of the form of stretched exponentials. The marked temperature dependence of the electron current function arises from the contribution of the equilibrium Boltzmann distribution, Eq. (32). The electron tunneling lifetime τ_{tun} was estimated from the approximate relation $I(\tau_{\mathrm{tun}})/I(0) = 1/e$. A central result of this analysis involves the temporal onset of electron tunneling [i.e., $I(t)=0.9$] at extremely long times [$t = 10^{10}$ s for $(^3\mathrm{He})_N$ at $T=2.5$ K and for $(^4\mathrm{He})_N$ at 4 K], with the extremely long values of the electron tunneling times in normal $(^4\mathrm{He})_N$ (at $T > T_\lambda$) and in $(^3\mathrm{He})_N$ clusters with $\tau_{\mathrm{tun}} = 10^{20}-10^{22}$ s

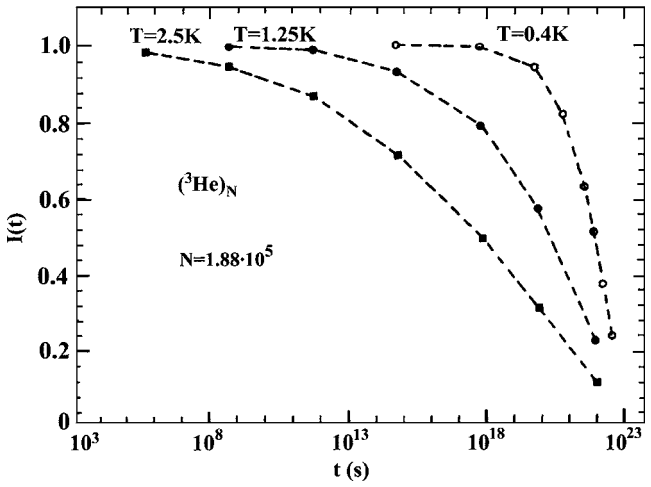

FIG. 4. The time dependence of the electron bubble survival probability $I(t)$ vs t, Eqs. (33) and (34), from a bubble located near the center in the normal fluid $(^3\mathrm{He})_N$ cluster ($N = 1.88\times 10^5$), at different temperatures marked on the curves.

(Fig. 4). These unphysically long lifetimes (which exceed the lifetime of the universe) for electron escape times from normal helium clusters constitute only rough estimates of the upper limits for these observables as other dynamic processes will result in the annihilation of the negative helium cluster on such time scales. The results of these lifetime calculations demonstrate that electron tunneling from a bubble in a normal fluid cluster is so long that it is not amenable to experimental observation under any real-life conditions. These conclusions concur with previous analyses of the static model[4,5] that used the flat surface tunneling probability[23] and are in accord with experimental work.[3,6–8]

B. Fast electron tunneling from superfluid helium clusters

The negligible dissipation effects for the bubble motion in superfluid clusters, which are characterized by exceedingly long damping times of $\tau_D \simeq 10$ s (Sec. IV), induce a free oscillatory bubble motion in the image potential with a short oscillation lifetime of $\tau_0 \sim 10^{-9}-10^{-10}$ s. Electron bubbles initially produced in the physically acceptable region 30 Å $\leqslant d \leqslant$ 50 Å (Sec. IV) in the superfluid cluster will manifest tunneling during the undamped oscillatory translational motion in the image potential.[8,22] We consider an electron bubble initially located at the radial distance d from the cluster boundary. The dynamic spatial distribution $p_f(r)$ of the electron bubble in the image potential in the absence of dissipation can be described by the tunneling probability from the bubble location at distances $-d \leqslant r \leqslant d$ from the cluster surface, where the bubble moves back and forth from $-d$ up to d in the image potential.

The dynamic radial distribution of the electron bubble in the cluster is

$$p_f(r) = |y/v(r)|, \tag{35}$$

where

$$v(r) = \{2[\epsilon - \bar{V}_{\rm im}(r)/M_B]\}^{1/2} \tag{35a}$$

and

$$y = \int dr\{2[\epsilon - \bar{V}_{\rm im}(r)]/M_B\}^{-1/2}, \tag{35b}$$

with $\bar{V}_{\rm im}(r)$ being given by Eq. (26). ϵ is the initial energy in the image potential, $v(r)$ is the velocity of the bubble motion with its center at distance R from the cluster center, and y is the period of the bubble oscillation. In this case the electron bubble survival probability $I(t)$ in the cluster assumes the form

$$I(t) = \int_{-d}^{d} p_f(r)\exp(-\phi(r)t)dr, \tag{36a}$$

where $\phi(r)$ is given by Eqs. (10a) and (11). Moreover, the major contribution to the electron escape is from the narrow range $d \cdots (d-\Delta d)$, where $\Delta d/d < 1$. On the basis of the exponential distance dependence of $\phi(d)$, we (arbitrarily but physically) choose Δd from the reduction of ϕ by two orders of magnitude, i.e., $\phi(d-\Delta d)/\phi(d) = 0.01$, so that

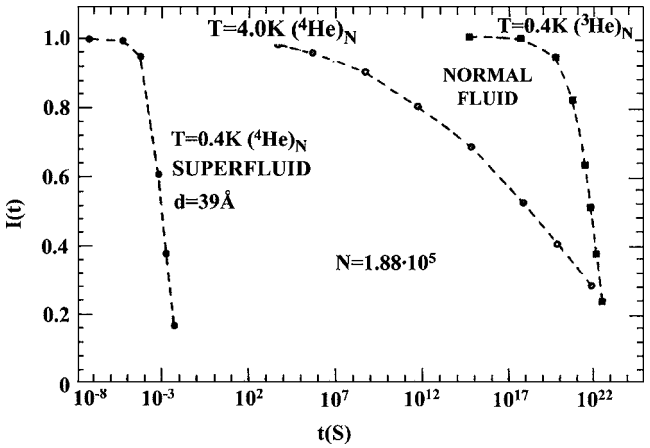

FIG. 5. The dependence of $I(t)$ on t, Eqs. (35), (36a), and (36b), for a superfluid $(^4\text{He})_N$ cluster ($N = 1.88 \times 10^3$) presented for a temperature of $T = 0.4$ K for an initial distance $d = 39$ Å. These data are compared with the $I(t)$ dependence on t for normal $(^3\text{He})_N$ ($T = 0.4$ K) and superfluid $(^4\text{He})_N$ ($T = 4.0$ K) clusters. (NORMAL FLUID) represents normal fluid clusters while (SUPERFLUID) represents superfluid clusters.

$\Delta d = 4.4/\beta \approx 4.4$ Å. We then calculate the integral, Eqs. (36a) and (36b), in the range $(d-\Delta d)\cdots d$,

$$I(t) = \int_{d-\Delta d}^{d} p_f(r)\exp(-\phi(r)t)dr. \tag{36b}$$

In Fig. 5 we portray the results of model calculations for the time dependence of $I(t)$, based on Eqs. (5), (7b), (10b), (35), and (36a), for superfluid $(^4\text{He})_N$ clusters with $N = 1.88 \times 10^5$ at $T = 0.4$ K. These calculations were performed for $d = 39$ Å, which falls well in the physically acceptable region of d. This $I(t)$ versus t curve exhibits a near-exponential decay with time, with the characteristic lifetime $\tau_{\rm tun} \simeq 10^{-2}$ s for electron tunneling. In Fig. 5 we compare the current decay curve $I(t)$ versus t for $(^4\text{He})_N$ superfluid clusters ($N = 1.88 \times 10^5$) with the $I(t)$ versus t curves for normal fluid clusters of the same size, i.e., $(^3\text{He})_N$ at $T = 0.4$ K and $(^4\text{He})_N$ at $T = 4.0$ K, calculated by the procedure of Sec. V A. The huge, 22 orders of magnitude, difference between the electron tunneling times from electron bubbles in superfluid clusters and in normal fluid clusters demonstrates the role of electron bubbles to interrogate the unique differences in the transport of this nanoprobe in the superfluid and in the normal fluid.[8,22]

VI. COMPARISON WITH EXPERIMENT

The exceedingly long tunneling times from electron bubbles in normal fluid $(^3\text{He})_N$ and $(^4\text{He})_N$ clusters are consistent with the experimental results of Toennies and co-workers,[3,6–8] who did not detect electron emission from electron bubbles in large normal fluid $(^3\text{He})_N$ clusters. One concludes that detachment of electron bubbles cannot be observed from normal fluid large clusters and is amenable to experimental observation only for superfluid large clusters.[3,6–8]

In further calculations of $\tau_{\rm TUN}$ we utilized a more elaborate expression for the tunneling lifetimes,

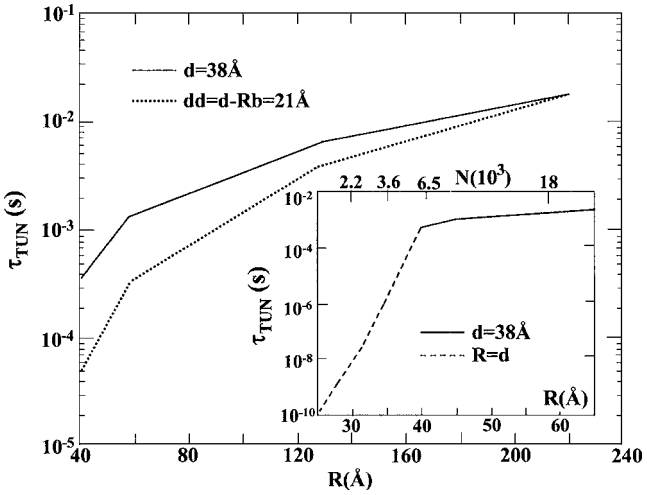

FIG. 6. Cluster size dependence of electron tunneling lifetimes τ_{TUN}, Eq. (37), for superfluid $(^4He)_N$ clusters (T=0.4 K). The cluster size was varied in the range R=41.5–222 Å ($N=6.5\times10^3-10^6$). Calculations were performed for fixed values of d=38 Å (solid curve) and of dd=21 Å (dotted curves). The inset shows these τ_{TUN} data for $R>41.5$ Å at a fixed d =38 Å (solid curve) and the τ_{TUN} for tunneling from a "helium balloon" with the bubble center coinciding with the cluster center, and $d=R$, with d decreasing with decreasing R.

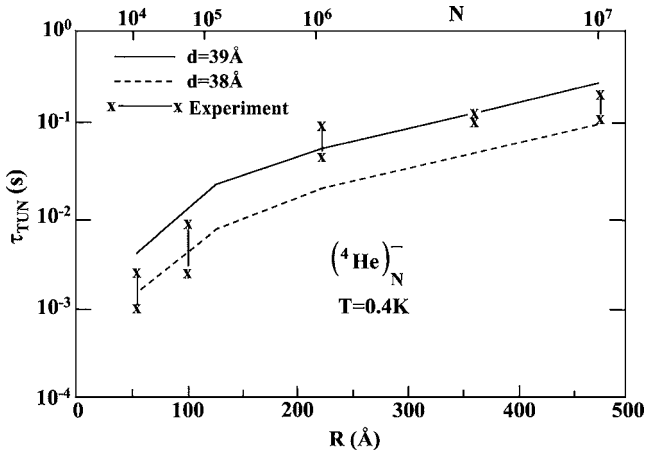

FIG. 7. Lifetimes for electron tunneling from superfluid $(^4He)_N$ clusters (T=0.4 K). The τ_{TUN} data were calculated in the cluster size domain $N=10^4-10^7$. Theoretical results are presented for d=39 Å (solid curve) and for d=38 Å (dashed curve). The lengthening of τ_{TUN} with increasing the cluster size (at a fixed value of d) is traced to cluster curvature effects on electron tunneling dynamics (see text). The experimental data (x—x) for the times of electron detachment times from superfluid $(^4He)_N$ clusters (Ref. 8) are marked on the panel.

$$\tau_{TUN} = |I(t)/(dI(t)/dt)| \quad \text{at } I(t)/I(0) = 1/e. \tag{37}$$

The tunneling lifetimes were calculated for electron bubbles in superfluid $(^4He)_N$ clusters in the size domain $N=6.5\times10^3-10^7$ (R=41.5–478 Å) with the cluster size dependent bubble radii R_b=13.5–17.0 Å.[27] The initial distance d for the location of the bubble (Fig. 1) constitutes a fitting parameter in these model calculations and was taken in the range d =38–39 Å. This value of d is somewhat lower than, but comparable to, the thermalization distance L=50 Å of electrons in macroscopic liquid helium.[19] We also assumed that in the cluster size domain studied herein d is independent of the cluster size.

In Fig. 6 we present the cluster size dependence of the electron tunneling times for the shortest bubble center-cluster surface distance of d=38 Å. In Fig. 6 we also included the results of model calculations for a fixed value of the shortest tunneling barrier width $dd=d-R_b$=21 Å. The data for electron tunneling dynamics reveal a marked increase of τ_{TUN} with increasing R, with a two orders of magnitude increase of τ_{TUN} in the cluster size domain R=41.5 Å (N=6500)$-R$ =222 Å ($N=10^6$). This lengthening of the lifetime (at fixed d) with increasing the cluster radius manifests the effects of cluster size and curvature on the electron tunneling dynamics. The cluster size dependence of τ_{TUN} at a fixed value of dd manifests a similar trend with that of the τ_{TUN} versus d dependence, with a more marked decrease of τ_{TUN} at lower values of R, which can be traced to the decrease of the bubble radius for small clusters. In what follows, the electron tunneling dynamics at a fixed value of d=38–39 Å will be explored. Calculations for τ_{TUN} from a bubble, whose center is displaced from the cluster center, are adequate for $R>d$, i.e., down to $R\simeq d+2r_0$, where r_0 is the radius of the helium atom. These calculations were performed down to R =41.5 Å (N=6500). For small cluster sizes (i.e., for cluster radii below R=41.5 Å) we calculated τ_{TUN} from a "helium balloon" with the bubble center coinciding with the cluster center, i.e., setting $d=R$. The tunneling times in the range R=41–26 Å were calculated from Eqs. (5), (6), and (24) and are characterized by the decrease of the d ($=R$) values and with the decrease of the barrier width $d-R_b$ with decreasing R. Accordingly, $\tau_{TUN}=\exp(\beta R)$ in this range (inset to Fig. 6). For large cluster sizes of $R\geqslant41.5$ Å, d is kept fixed and τ_{TUN} exhibits a weaker algebraic cluster size dependence, due to cluster curvature effects (inset to Fig. 6).

In Fig. 7 we present the results of our model calculations for the cluster size dependence of τ_{TUN} for fixed values of d=38 Å and d=39 Å. These calculated tunneling times are in good agreement with the experimental results,[8] as is apparent from Fig. 7. This concurrence between theory and experiment[8] demonstrates the role of cluster size effects and cluster curvature effects on electron tunneling dynamics. Of course, our model calculations of τ_{TUN} for a superfluid cluster rest on a simplified description of the electron bubble, disregard structural and energetic changes arising from the dislocation of the bubble from the cluster center, and use the initial distance d as a fitting parameter. Further refinements of extensions of the theory of electron tunneling dynamics from bubbles in superfluid clusters will be of interest. These will involve the following amendments and additions: (i) the effects of the bubble diffuseness and the cluster surface profile on the electron tunneling; (ii) a treatment of small local changes in energetics, structure, and charge distribution of the electron bubble, when it is dislocated from the cluster center; (iii) examination of the implications of an inhomogeneous distribution of the initial bubble distance d on the current decay curves; (iv) the nuclear dynamics of compression of the empty bubble,[21] sequentially with electron tunneling; (v) studies of the role of nuclear Franck-Condon factors on the electron tunneling process; and (vi) the exploration of the implications of the intermediate thermal relaxation time fall-

ing between the slow limit and the fast limit in $(^4He)_N$ clusters below the lambda point, but close to T_λ, where the superfluid fraction is finite but lower than unity, so that the viscosity assumes a mean value between the superfluid and the normal fluid properties. These refinements and extensions of the theory will be of considerable interest, however, they will not change the general conclusions emerging from the present work.

VII. CONCLUDING REMARKS

The experimental results for electron detachment from $(He)_N^-$ superfluid clusters,[3,6–8,17] in conjunction with the present analysis, reflect on the role of electron bubbles as microscopic probes for superfluidity of finite boson quantum clusters. Electron tunneling from bubbles is grossly affected by the distinct mode of motion of the electron bubble, which is dissipative in normal fluid $(^4He)_N$ and $(^3He)_N$ clusters and undamped in superfluid $(^4He)_N$ clusters. The huge difference in the motional damping times of the electron bubble, i.e., $\tau_D \simeq 4\times 10^{-12}$ s for the normal fluid cluster and $\tau_D \simeq 10$ s for the superfluid cluster, will induce electron tunneling from the electron bubble located in the vicinity of the center of the normal fluid cluster and from the electron bubble located near the bubble boundary of the superfluid cluster. These distinct locations of the bubble during electron tunneling will result in exceedingly long tunneling lifetimes ($\tau_{TUN} \sim 10^{20}$ s) for normal fluid clusters and short lifetimes ($\tau_{TUN} \sim 10^{-3}-10^{-1}$ s) for superfluid clusters. The theoretical exploration of the electron bubble translational motion in the image potential within normal fluid and superfluid clusters allows us to infer on the dramatic effects of superfluidity in large finite boson quantum clusters using the techniques of electron detachment.

In the exploration of the dynamics of electron tunneling from bubbles in superfluid and normal fluid $(^4He)_N$ and $(^3He)_N$ clusters, we focused on clusters in the size domain of $N=6.5\times 10^3-10^7$. An interesting question in the realm of quantum size effects pertains to threshold size effects,[15] e.g., what is the minimal helium cluster size for the support of an excess electron bubble? From the analysis of the energetic stability of the electron bubble in $(He)_N$ clusters (Paper I),[27] we concluded that the minimal cluster for which the electron bubble is energetically stable corresponds to $N\simeq 5200$. We have already pointed out that dynamic effects involving electron tunneling of the bubble may result in the depletion of the energetically stable electron bubble state on the experimental time scale t_{exp} for the interrogation of $(He)_N^-$ clusters [$t_{exp} \gtrsim 10^{-6}$ s (Refs. 3 and 6–8)]. Accordingly, the dynamic stability criterion is governed by the experimental conditions for the detachment of an excess electron from $(He)_N^-$ clusters. We infer that dynamic stability will prevail for $\tau_{TUN} > 10^{-6}$ s. As we are concerned here with electron tunneling from moderately small $(He)_N$ clusters, we shall consider electron tunneling from a centrally located bubble (a "helium balloon") in these moderately small clusters. From the τ_{TUN} data presented for $d=R$ (inset of Fig. 6), we conclude that the minimal cluster radius for dynamic stability, i.e., $\tau_{TUN}=10^{-6}$ s, is realized for $R=35$ Å. For this value of R we infer that dynamic stability is ensured for $N=[(R)^3-(R_b^e)^3]/r_0^3$, where $R_b^e \simeq 13.5$ Å, as appropriate for an "electron balloon" in small clusters (Paper I). The lowest cluster size for dynamic stability of the electron bubble is $N\simeq 3800$. This minimal cluster size, which satisfies the constraints of dynamic stability, should be compared with the onset of energetic stability, which was estimated to be $N=5200$ (Paper I). In view of the uncertainty of the estimates of the energetic and dynamic stability onsets we conclude that the electron bubble in $(^4He)_N$ clusters will be amenable to experimental observation for $N=4500\pm 700$, with the lower and upper limits marking the dynamic threshold and the energetic stability threshold, respectively. This prediction provides an interesting avenue for the experimental search for the lowest cluster size allowing for electron localization in a "helium balloon" which supports a localized excess electron.

ACKNOWLEDGMENTS

We are grateful to Professor J. P. Toennies for stimulating discussions and correspondence. This research was supported by the German-Israeli James Franck Program on Laser-Matter Interaction.

[1] L. Meyer and F. Reif, Phys. Rev. **119**, 1164 (1960).
[2] R. Krishna and K. B. Whaley, J. Chem. Phys. **93**, 746 (1990).
[3] M. Farnik, U. Henne, B. Samelin, and J. P. Toennies, Phys. Rev. Lett. **81**, 3892 (1998).
[4] T. Jiang, C. Kim, and J. A. Northby, Phys. Rev. Lett. **71**, 700 (1993).
[5] J. A. Northby, C. Kim, and T. Jian, Physica B **197**, 426 (1994).
[6] U. Henne and J. P. Toennies, J. Chem. Phys. **108**, 9327 (1998).
[7] M. Farnik, B. Samelin, and J. P. Toennies, J. Chem. Phys. **110**, 9195 (1999).
[8] M. Farnik and J. P. Toennies, J. Chem. Phys. **118**, 4176 (2003).
[9] M. Anderson, J. Ensher, M. Matthews, C. Wieman, and E. Comell, Science **269**, 198 (1995).
[10] K. Davis, M.-O. Mewes, M. R. Andrews, W. J. van Druten, D. S. Durfee, D. M. Kurn, and W. Ketterle, Phys. Rev. Lett. **75**, 3969 (1995).
[11] C. Bradley, C. Sackett, J. Tollet, and R. Hulet, Phys. Rev. Lett. **78**, 985 (1997).
[12] P. Sindzingre, M. L. Klein, and D. M. Ceperley, Phys. Rev. Lett. **63**, 1601 (1989).
[13] E. L. Pollock and K. J. Runger, Phys. Rev. B **46**, 3535 (1992).
[14] J. Jortner, J. Chem. Phys. **119**, 11335 (2003).
[15] J. Jortner and M. Rosenblit, Adv. Chem. Phys. **132**, 247 (2006).
[16] V. L. Ginzburg and A. A. Sobyanin, Sov. Phys. Usp. **19**, 773 (1977).
[17] K. Martini, J. P. Toennies, and C. Winkler, Chem. Phys. Lett. **178**, 429 (1991); M. Hartmann, F. Mielke, J. P. Toennies, A. F. Vilesov, and G. Benedek, Phys. Rev. Lett. **76**, 4560 (1996).
[18] S. Grebenev, J. P. Toennies, and A. F. Vilesov, Science **279**, 2083 (1998).
[19] D. G. Onn and M. Silver, Phys. Rev. **183**, 295 (1969).
[20] M. Rosenblit and J. Jortner, Phys. Rev. Lett. **75**, 4079 (1995).
[21] M. Rosenblit and J. Jortner, J. Phys. Chem. A **101**, 751 (1997).
[22] M. Rosenblit and J. Jortner (unpublished).
[23] W. Schoepe and G. W. Rayfield, Phys. Rev. A **7**, 2111 (1973).
[24] M. W. Cole and J. R. Klein, J. Low Temp. Phys. **36**, 331 (1979).
[25] F. Ancilotto and F. Toigo, Phys. Rev. B **50**, 12820 (1994).
[26] J. Bardeen, Phys. Rev. Lett. **6**, 57 (1961).
[27] M. Rosenblit and J. Jortner, J. Chem. Phys. **124**, 194505 (2006), preceding paper.
[28] J. Poitrenaud and F. I. B. Williams, Phys. Rev. Lett. **29**, 2130 (1972); **32**, 1213(E) (1974).
[29] J. Wilks, *Liquid and Solid Helium* (Oxford University Press, Oxford, 1967).
[30] J. P. Toennies and A. F. Vilesov, Annu. Rev. Phys. Chem. **49**, 1 (1998).

[31] J. P. Toennies, A. F. Vilesov, and K. B. Whaley, Phys. Today **2**, 31 (2002).
[32] J. A. Northby, J. Chem. Phys. **115**, 10065 (2001).
[33] K. Callegari, K. K. Lehmann, R. Schmied, and G. Scoles, J. Chem. Phys. **115**, 10090 (2001).
[34] F. Stienkemeier and A. F. Vilesov, J. Chem. Phys. **115**, 10119 (2001).
[35] J. P. Toennies and A. F. Vilesov, Angew. Chem., Int. Ed. **43**, 2622 (2004).